STUDY OF STRAND CRITICAL CURRENT DEGRADATION IN A RUTHERFORD TYPE Nb_3Sn CABLE

E. Barzi,[1] C. Boffo,[1] D. R. Chichili,[1] J. P. Ozelis,[1]
R. M. Scanlan,[2] H. C. Higley,[2] and A. V. Zlobin[1]

[1] Fermi National Accelerator Laboratory
Batavia, Illinois 60510, USA
[2] Lawrence Berkeley National Laboratory
Berkeley, California 94720, USA

ABSTRACT

Fermilab is developing high field superconducting dipole magnets based on Nb_3Sn technology for a post-LHC very large hadron collider (VLHC). The first prototype is a 1 meter long dipole with a nominal field of 10-11 T. This model utilizes a 28-strand keystoned Rutherford-type superconducting cable. An important part of this project is the development and testing of the prototype cable. Multifilamentary Nb_3Sn strands of 1 mm diameter have been produced by IGC using the internal tin process. Short samples of Rutherford cable with four different packing factors, 90%, 91%, 91.6%, and 93%, have been fabricated at LBNL. After heat treatment, I_c measurements made on the round virgin strands were compared with those made on the strands extracted from cable samples. This paper presents studies of I_c degradation in the Nb_3Sn strands due to cabling.

INTRODUCTION

Within the framework of an R&D program towards a post-LHC very large hadron collider (VLHC), a high field Nb_3Sn dipole magnet (HFM) with a nominal field of 10-11 T is being developed at Fermilab.[1] The maximum field, B_{max}, is determined by the coil width and by the critical current density, J_c, of the superconductor. Hence, for a cost effective magnet design, J_c should be as high as possible.

The critical current, I_c, of the original virgin strand is reduced during magnet fabrication. Among the factors that reduce I_c are strand deformation during cabling, which occurs before reaction, and cable compression in the coil, which is applied after the magnet coils have been reacted.[2,3] This latter factor is due to J_c sensitivity of Nb_3Sn to strain.[4,5] This paper addresses I_c degradation issues related to cabling.

* Work supported by the U. S. Department of Energy.

SUPERCONDUCTING STRAND AND CABLE DESCRIPTION

Strand and cable parameters

The superconducting Nb_3Sn strand for the HFM prototype cable was produced by IGC using the internal tin process and the strand design developed for ITER.[6] Strand and cable geometrical parameters are summarized in Tables 1 and 2.

Table 1. Nb_3Sn strand parameters.

Parameter	Unit	Value
Strand diameter	mm	1.011±0.001
Number of subelements		61
Nb filament diameter	μm	4.1
Cu to non-Cu ratio		0.64:1
Twist pitch	mm	12±3

Table 2. Nb_3Sn cable parameters.

Parameter	Unit	Value
Number of strands, *n*		28
Strand diameter, *d*	mm	1.012±0.001
Cable width, *w*	mm	14.233
Keystone angle, *f*	degree	1.021
Lay angle, *y*	degree	14.53

Cable samples with different packing factors were fabricated at LBNL and extracted strands were tested at Fermilab. The packing factor, P, of a cable is defined as the ratio of the cross section occupied by the strands to the overall cross section of the cable:

$$P = \frac{npd^2}{2w(t_1 + t_2)\cos y} \quad , \qquad (1)$$

where t_1 and t_2 are the minor and major edge thicknesses. The other variables are defined in Table 2.

Different packing factors were obtained by varying the average cable thickness, which was 1.816 mm, 1.797 mm, 1.785 mm, and 1.758 mm, corresponding to packing factors of 90%, 91%, 91.6%, and 93% respectively.

Sample preparation and measurement procedure

For this study, two sets of samples were prepared, consisting of 8 and 6 units each. Each set included virgin (round) strands and strands extracted from the four cables. The samples were wound on grooved cylindrical barrels made of Ti-6Al-4V alloy, and held in place by two removable Ti-alloy end rings.[7] The two sets were heat treated in an argon atmosphere at various temperatures to form superconducting Nb_3Sn. A different thermal cycle was used for each set [HT-1 (nominal) and HT-2 (short)] to monitor the dependence of I_c degradation on heat treatment. The heat treatment schedule for the two cycles is given in Table 3.

Table 3. Heat treatment cycles.

	Heat treatment	Step 1	Step 2	Step 3	Step 4
Ramp rate, ^{o}C/h	HT-1 (nominal)	6	6	25	25
Temperature, ^{o}C		185	460	570	650
Duration, h		48	100	200	175
Ramp rate, ^{o}C/h	HT-2 (short)	-	-	25	25
Temperature, ^{o}C		-	-	575	750
Duration, h		-	-	200	18

After the reaction phase, the Ti-alloy end rings of the cylindrical barrels were replaced by copper rings, and voltage-current characteristics were measured in boiling He at 4.2 K and with a transverse magnetic field between 10 T and 15 T. Voltages were measured along the sample by means of voltage taps placed 50 cm apart. A typical voltage curve at 12 T and 4.2 K is shown in Figure 1. Additional voltage taps were placed on each side of the thick and of the thin edge of the extracted strands. The distance between these voltage taps was 6 cm.

The I_c was determined from the voltage curve using the 10^{-14} Ω·m resistivity criterion, as illustrated in Figure 1. By fitting this curve with the power law $V \sim I^n$, n-values were determined in the voltage range from V_c to $10 \cdot V_c$ at a given magnetic field, where V_c is the voltage corresponding to I_c.

TEST RESULTS AND DISCUSSION

Critical current measurements of virgin and extracted strands

The I_c results for the virgin and extracted strands for the nominal and the short thermal cycles are shown in Figures 2a), b) as a function of magnetic field. Some increasing I_c degradation is apparent in cables with increasing packing factors.

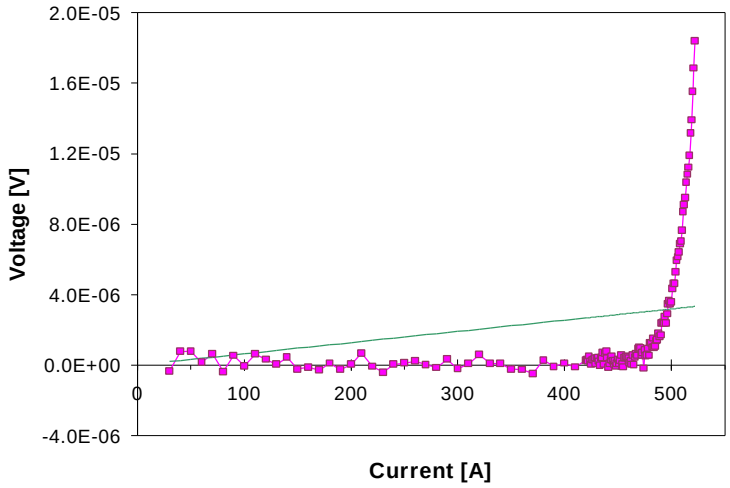

Figure 1. A typical voltage-current characteristic. The line illustrates the resistivity criterion used to determine I_c.

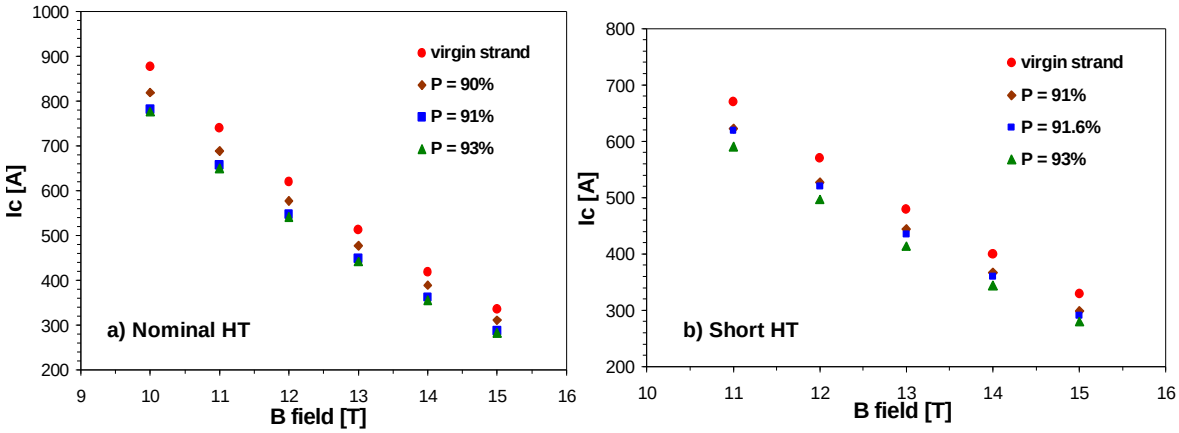

Figure 2. I_c dependence on field for the virgin and extracted strands.

The I_c degradation, expressed as the I_c of an extracted strand normalized to the I_c of the virgin strand, is shown in Figures 3a), b) as a function of field. This can also be written as:

$$\frac{I_c^{\,P}}{I_c^{\,vg}} = \frac{J_c^{\,P}(B)}{J_c^{\,vg}(B)} \cdot \frac{A_{Non-Cu}^{\,P}}{A_{Non-Cu}^{\,vg}}. \qquad (2)$$

It can be seen that the I_c degradation depends on B, with an indication of an increasing effect with higher packing factor and higher field.

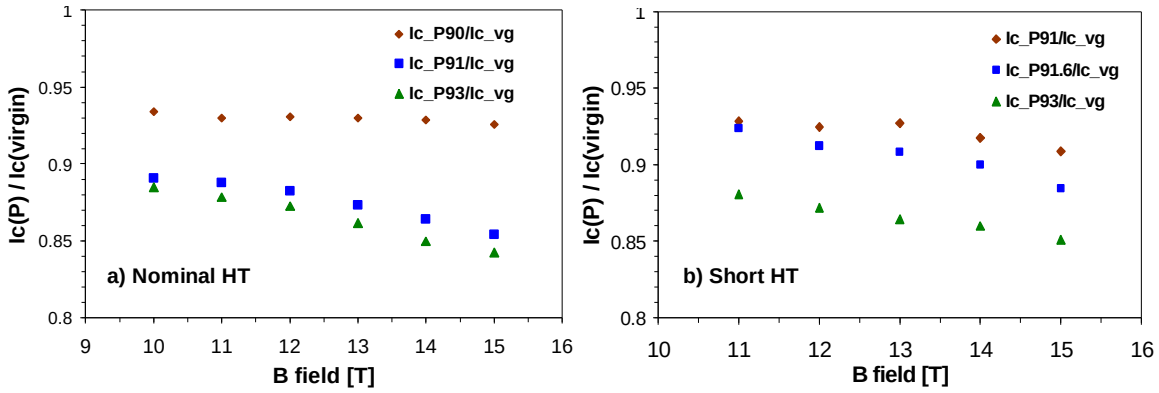

Figure 3. Normalized I_c as a function of magnetic field for extracted strands.

The I_c degradation as a function of the cable packing factor at a field of 12 T is shown in Figure 4. A normalized I_c of 1 is assigned to P=78.5%, which is the value of an undeformed round strand inscribed in a square. Results are presented for both sets of samples. No conclusive effect related to heat treatment can be determined.

The above results show that the I_c degradation due to cabling is relatively low for the cables made of internal tin Nb_3Sn strand. For the cable with the largest packing factor (93%), it is less than 13% at 12 T and less than 16% at 15 T, and it can be kept lower than 7% by choosing a cable with a packing factor below 90%. This effect is much smaller than that observed earlier in the cables made of PIT strands for the MSUT high field dipole.[2] However, it is comparable with the degradation of cabled NbTi strands.[8]

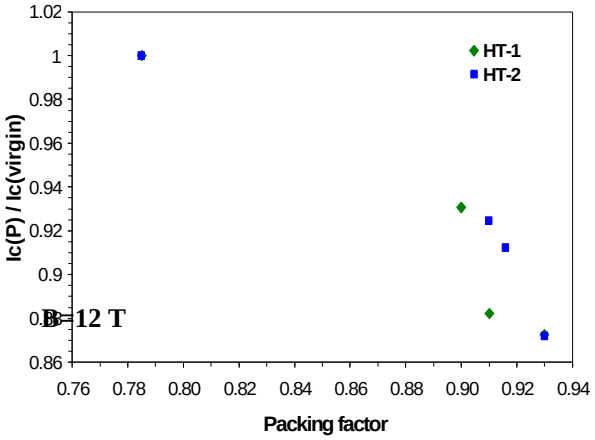

Figure 4. Effect of packing factor on I_c degradation due to cabling.

Discussion

To understand possible causes of I_c degradation after cabling, additional studies were performed.

Figures 5a), b) show the measured n-values of virgin and extracted strands for the nominal and the short thermal cycles as a function of magnetic field. The n-value is a quality factor related to the longitudinal uniformity of the superconducting filaments.[6] These high n-values indicate a very good uniformity of the virgin strand for both heat treatments. The n-value sensitivity to the cable packing factor appears to be low for the nominal reaction cycle. Its reduction is less than 5% at 12 T for the strand with the largest packing factor. On the other hand, in the same strand the n-value is reduced by half in the short cycle.

Figure 6 shows the results of magnetization measurements between zero field and 3 T of a virgin strand and of a strand extracted from the cable with the largest packing factor for the nominal cycle. The width of the magnetization loop is proportional to the local J_c in the superconductor. As can be seen, there is no observable J_c degradation at low fields. The AC losses (loop area) were 436.9±1.3 kJ/m^3 for the virgin strand, and 438.6±2.6 kJ/m^3 for the extracted strand, *i.e.* practically the same. The magnetization measurements hint that J_c degradation may be localized in rather small areas along the strand. This is qualitatively consistent with the I_c measurements that were performed on the thick and thin edges of the extracted strands.

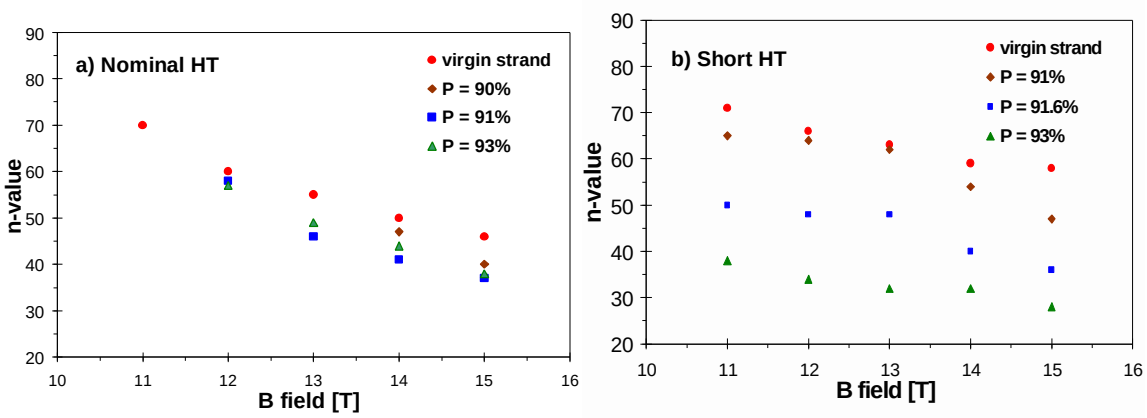

Figure 5. n-values vs. magnetic field for virgin and extracted strands.

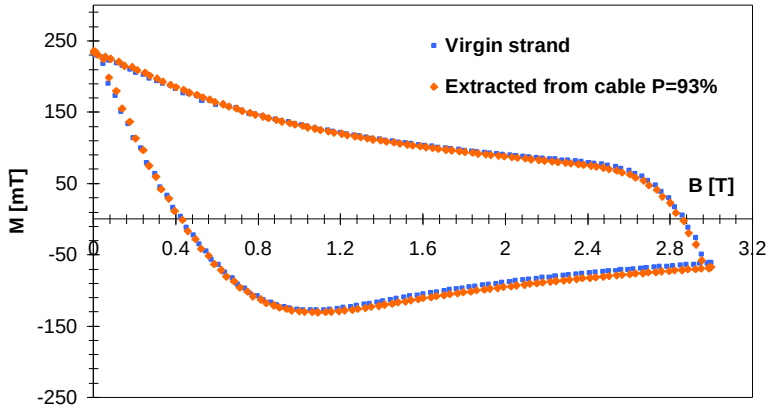

Figure 6. Magnetization loops for the virgin and the extracted strand with P=93% for the nominal cycle.

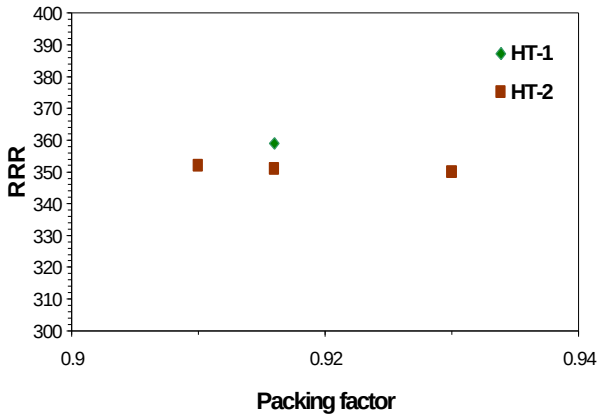

Figure 7. RRR as function of packing factor.

In order to further understand the possible causes of I_c degradation due to cabling, the following additional parameters were studied:

a) damage of the diffusion barrier and tin leakage into the outer copper, by measuring the copper residual resistivity ratio (RRR);
b) non-uniformity of Sn diffusion in the deformed part of the strand cross section, by performing a point to point compositional analysis of the Cu-Sn matrix and of the Nb-Sn filaments by energy dispersion X-rays (EDX);
c) strand cross section reduction at cable edges, by measuring the cross sectional areas of virgin and extracted strands on their SEM pictures.

Shown in Figure 7 is the RRR (at zero magnetic field) as a function of cable packing factor for the extracted strands. The RRR for the virgin strand was specified to be at least 300. These data show no significant effect due to packing factor and indicate that the diffusion barrier is not damaged to the point where tin contamination of the copper stabilizer occurs.

SEM pictures of the cross sections of a virgin strand, of a straight segment of an extracted strand (P=93%) at its middle point, at one of its thick edges, and at one of its thin edges are shown in Figures 8A), B), C), and D) respectively for the nominal cycle. A compositional analysis was performed by EDX on these cross sections at a majority of the points shown. No significant differences are seen

between the virgin and the extracted strand cross sections, either in the Cu-Sn matrix composition or in the completeness of the Nb filaments reaction. The long thermal cycle used for these strands allowed a full reaction of the Nb filaments throughout the entire cross sectional area even in the most deformed parts. Tin diffusion also appeared to be uniform since the tin left in the Cu-Sn matrix after reaction was around 3±1 atomic% throughout the matrix. The virgin and the extracted strands may show a difference in the short thermal cycle though, where tin diffusion and reaction of the Nb filaments could occur inhomogeneously along the strand, and more so in the presence of necking. This could explain the large n-value degradation of the extracted strands in the short cycle, shown in Figure 5b) above.

Cross sectional area and thickness of the major components of the virgin and extracted strands were measured for the nominal cycle using image analysis software. Results of these measurements, including cross sections of the total area, of the non-copper area, and of the diffusion barrier area, are summarized in Table 4. The non-copper area at the middle section of a straight segment is reduced by 13.5%. This should contribute a proportional decrease in I_c under the assumption that the average area reduction is close to the area reduction at the middle section between edges. The thickness of the diffusion barrier was about 14 μm in the virgin strand, and reached a minimum of 3 μm in the most deformed part of an edge.

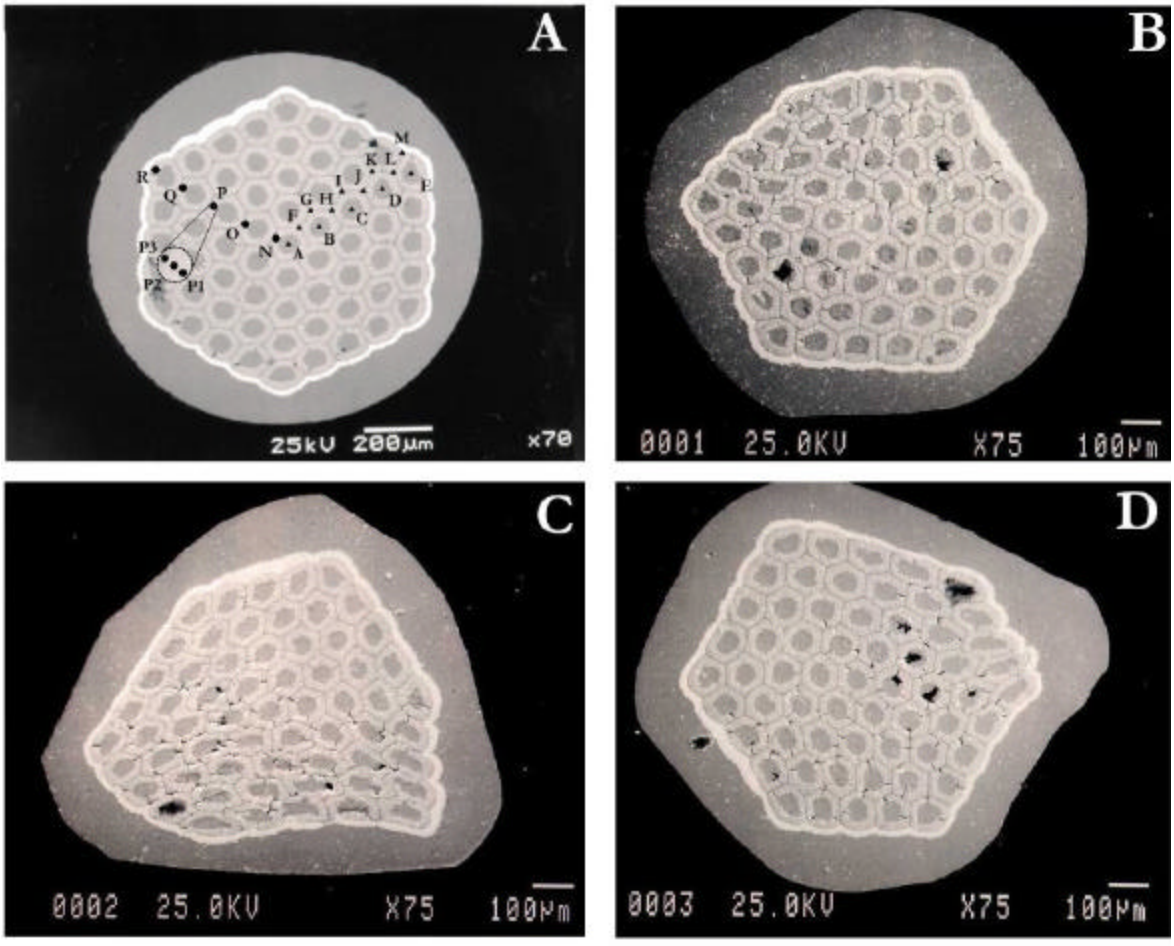

Figure 8. SEM pictures of strand cross sections for the nominal thermal cycle: A) virgin; B) middle section of straight segment, C) thick edge, and D) thin edge of extracted strand with P=93%.

Table 4. Cross sectional areas of virgin and extracted strands.

Cross section	Virgin	Straight section	Thick edge	Thin edge
Total, mm^2	0.97	0.86	0.77	0.83
Non-Cu, mm^2	0.59	0.51	0.46	0.48
SC, mm^2	0.54	0.45	0.41	0.43
Copper, mm^2	0.38	0.35	0.31	0.35
Barrier, mm^2	0.05	0.06	0.05	0.05

SUMMARY

Based on the above studies, the cross section of the cable for the first Fermilab Nb_3Sn short model was chosen. The data showed that for Nb_3Sn strands produced by the internal tin process, the I_c degradation after cabling should be less than 5% if the cable packing factor does not exceed 88%. I_c cabling degradation can be explained by a reduction in the strand cross sectional area after cabling.

Continued study of cable degradation for Nb_3Sn strands fabricated using different technologies (IT, MJR and PIT) will be pursued.

ACKNOWLEDGMENT

The authors are grateful to Peter Limon for his interest and continuous support.

REFERENCES

1. G. Ambrosio et al., "Conceptual Design of the Fermilab Nb_3Sn High Field Dipole Model", PAC'99, New York, NY, USA, March 1999.
2. A. den Ouden, S. Wessel, E. Krooshoop, R. Dubbeldam, and H. H. ten Kate, "An experimental 11.5T Nb_3Sn LHC type of dipole magnet", *IEEE Trans. On Magnetics*, Vol. 30, No. 4, July, 1994.
3. H. W. Weijers, H. H. J. ten Kate, J. M. van Oort, "Critical current degradation in Nb3Sn cables under transverse pressure", *IEEE Trans. On Applied Superconductivity*, Vol. 3, 1993, p. 1334.
4. J. W. Ekin, Cryogenics **20**, 611 (1980).
5. B. ten Haken, A. Godeke, and H. H. J. ten Kate, "The strain dependence of the critical properties of Nb_3Sn conductors", Journal of Applied Physics, Vol. 85, no. 6. March 15, 1999.
6. E. Gregory, E. Gulko, T. Pyon, and L. F. Goodrich, "Properties of internal tin Nb_3Sn strand for the International Thermonuclear Experimental Reactor", Advances in Cryogenic Engineering, Vol. 42, Plenum Press, New York, 1996.
7. L. F. Goodrich, J. A. Wiejaczka, A. N. Srivastava, T. C. Stauffer, "Superconductor critical current standards for fusion applications", NISTIR 5027, NIST.
8. V. Y. Fil'kin, et. al. , "Composite superconductors for UNK magnets", ICFA '86, p. 56, BNL, 1986.